Monograph:

Guo, Y., Zhao, Y., Billings, S.A. et al. (2009) Identification of excitable media using a scalar coupled map lattice model. Research Report. ACSE Research Report no. 1001 . Automatic Control and Systems Engineering, University of Sheffield

Identification of Excitable Media Using A Scalar Coupled Map Lattice Model

Yuzhu Guo, Yifan Zhao, S. A. Billings, Daniel Coca, R. I. Ristic and L. L. DeMatos

Research Report No. 1001

Department of Automatic Control and Systems Engineering
The University of Sheffield
Mappin Street, Sheffield,
S1 3JD, UK

10 August 2009

Identification of Excitable Media Using A Scalar Coupled Map Lattice Model

Yuzhu Guo[1], Yifan Zhao[1], S. A. Billings[1], Daniel Coca[1],

R. I. Ristic[2] and L. L. DeMatos[2]

[1] Department of Automatic Control and Systems Engineering

[2] Department of Chemical and Process Engineering

University of Sheffield

Abstract

The identification problem for excitable media is investigated in this paper. A new scalar coupled map lattice (SCML) model is introduced and the orthogonal least squares algorithm is employed to determinate the structure of the SCML model and to estimate the associated parameters. A simulated pattern and a pattern observed directly from a real Belousov-Zhabotinsky reaction are identified. The identified SCML models are shown to possess almost the same local dynamics as the original systems and are able to provide good long term predictions.

Keywords: Identification, excitable media, scalar coupled map lattice models, orthogonal least squares.

1 Introduction

Excitable media widely exists in chemical, physical and biological systems. A variety of patterns have been observed in excitable media such as: solitary, target-like patterns, spiral waves, and so on. These phenomena result from the interplay between local dynamics and diffusive transport. Therefore, excitable media are usually described using a reaction-diffusion equation. The reaction part provides the local dynamics and the diffusion part provides propagation of information.

A general reaction diffusion system has the form

$$\frac{\partial \mathbf{u}}{\partial t} = \mathbf{D}\nabla^2 \mathbf{u} + \mathbf{f}(\mathbf{u}, \mathbf{p}) \tag{1}$$

where **u** is a vector representing quantities of the components. The first term on the right hand side represents diffusion, with **D** a matrix of diffusion coefficients, and the second term represents local dynamics with kinetic parameters **p** (Maini et al. 1997).

Cells in excitable media can be characterised by three states: resting, excited and refractory. A cell in a resting state is stable for a small perturbation while a perturbation with strength greater than a certain threshold can cause this cell to undergo a large excursion. Usually, the shape of the generated response does not depend on the perturbation strength, as long as the perturbation exceeds the threshold. After this strong response, the system returns to its initial resting state. A subsequent excitation can be generated after a suitable length of time, called the refractory period, has passed. (Zykov 2008)

Mapping the continuous coupled partial differential equations into a discrete lattice produces the coupled map lattice model. Owing to the computational efficiency and richness of their dynamical behaviour, CML models have been widely used to study excitable media (Kaneko 1990). Cellular automata models which simplify the dynamic description of a system by mapping the systems behaviour onto a few discrete states can also be used to describe excitable media systems. In cellular automata models, the continuous effects of diffusion are mapped to simple rules based on neighbourhood interactions. Cellular neural networks (CNN) have also been shown to be another powerful model for the simulation of excitable media (Jankowski and Wanczuk 1994).

Excitable media have been extensively studied in many diverse fields including theoretical analysis, experiments and numerical simulations. However, most of these studies are focused on forward problems. That is, known models are used to describe and analyse the dynamical behaviours of excitable media systems. But in practice these models will often not be known. Finding the models is difficult and is referred to as the backward or the inverse problem. Therefore, identification of a model directly from observed spatio-temporal patterns is crucial for the study of excitable media. Until now, only a few results have been published on the inverse problem. Coca and Billings identified a spatiotemporal system directly from data using a coupled map lattice model(2001). Pan and Billings identified the Turing patterns using a similar model(2008). In both papers the prediction patterns were highly consistent to the original patterns. However, all information about the components which were involved in the evolution of the pattern was assumed to be measurable. This may be impractical for many real systems, such as, patterns in the Belousov-Zhabotinsky reaction and skin patterns on various fishes and shells, for example.

Zhao and Billings et al. identified a practical pattern acquired from a real Belousov-Zhabotinsky reaction using a type of cellular automata model, the Greenberg-Hasting model (GHM)(2007a). On the one hand, the GHM is a simple cellular automata model for the simulation of excitable media, on the other hand only three key parameters can be controlled when the neighbourhood is determined. Accordingly, it may be difficult to obtain a precise description of practical systems based on this model. Wei and Billings et al. identified a practical BZ pattern using a lattice dynamical wavelet neural network (LDWNN) model(2009). As in the GHM model used by Zhao and Billings, only one measured component was included in the LDWNN model, and only short term predictions were analysed.

In this paper excitable media are simulated in section 2 using both PDE and cellular automata models. A brand new model is proposed in section 3 for the identification of excitable media, the new model will be called the scalar coupled map lattice model (SCML). As a coupled map lattice model, this model is easy to use for the simulation of the system. Only one component measured directly from the spatio-temporal patterns is included, however the new model appears to be very useful in the identification of practical systems. By combining the new model with the powerful orthogonal least squares algorithm (Billings et al. 1989; Chen et al. 1989), a new identification method is proposed in section 4. A numerically simulated pattern from a coupled PDE model and a pattern acquired from a real chemical reaction are identified to illustrate this new method. The conclusions are finally given in section 5.

2 Simulations of Excitable Media

In this section two partial differential equation models and a cellular automata model are simulated to demonstrate what model properties produce typical patterns, and dynamical behaviours of excitable media.

2.1 Discretisation Method and Boundary Conditions

Traditionally, excitable media have been simulated by discretisation of the governing Partial Differential Equations (PDE). The forward-time centred space (FTCS) discretisation method is the simplest and most commonly used discreteisation method.

The first-order temporal derivative can be discretised as

$$\frac{\partial u(x,t)}{\partial t} \rightarrow \frac{u(x,t+\Delta t)-u(x,t)}{\Delta t} \tag{2}$$

For the spatial derivative, use

$$\frac{\partial u(x,t)}{\partial x} \rightarrow \frac{u(x+\Delta x,t)-u(x,t)}{\Delta x} \tag{3}$$

$$\frac{\partial^2 u(x,t)}{\partial x^2} \rightarrow \frac{u(x+\Delta x,t)-2u(x,t)+u(x-\Delta x,t)}{(\Delta x)^2} \tag{4}$$

Further, the Laplace operator can be discretised on the grid lattice sites as equation (5) for a von Neumann neighbourhood.

$$\nabla^2 u(i,j,t) = \frac{1}{(\Delta x)^2}\Big(\big(u(i+1,j,t)+u(i-1,j,t)+u(i,j+1,t)+u(i,j-1,t)\big)/4-u(i,j,t)\Big) \tag{5}$$

where (i,j) represents the spatial coordinate and t represents the time instant.

Different definitions of the boundary conditions for coupled partial differential equations can be used in simulations. Three of these boundary conditions which are commonly used in the simulations are: zero boundary conditions, periodic boundary conditions, and zero-flux boundary conditions.

2.2 Simulation of FitzHugh-Nagumo Model

A simple mathematical model for excitable media is the FitzHugh-Nagumo (FHN) model (FitzHugh 1955) of excitation in nerve and muscle tissue:

$$\begin{cases} u_t = D_u \nabla^2 u - u(u-1)(u-\alpha) - v \\ v_t = D_v \nabla^2 v + \varepsilon(\beta u - \gamma v - \delta) \end{cases} \quad (6)$$

The variables (u,v) interact locally according to the ordinary differential equations $\frac{du}{dt} = f(u,v)$ and $\frac{dv}{dt} = g(u,v)$, where $f(u,v) = -u(u-1)(u-\alpha) - v$, $g(u,v) = \varepsilon(\beta u - \gamma v - \delta)$. The nullclines for function f and g have the characteristic shape shown in Fig 1 (a) (the solid curves). In this model, there is a resting state (fixed point) where the nullclines intersect. A small perturbation is damped out (the dotted curve in Fig 1), but a perturbation over a certain threshold triggers a long excursion (the dashed curve in Fig 1). This is the typical dynamical behaviour of excitable media. Fig 1 (b) shows the response of the system for perturbations with different strengths.

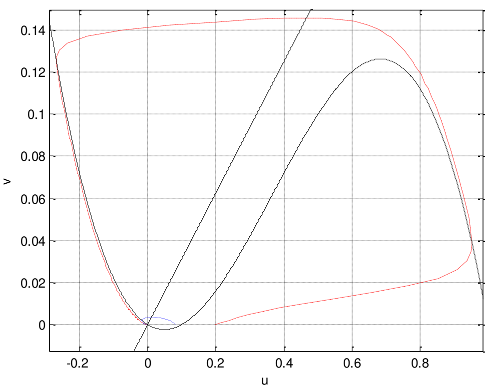

(a)

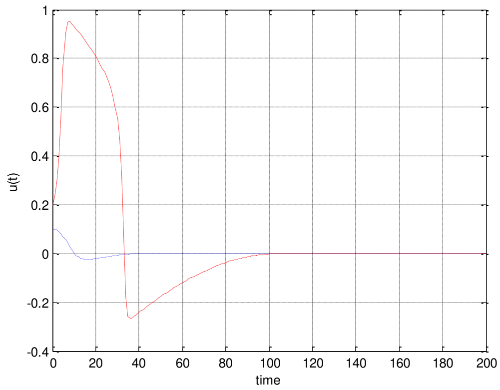

(b)

Fig 1 Local dynamics of the FitzHugh-Nagumo model

with $\alpha = 0.1, \beta = 0.5, \gamma = 1.6, \delta = 0, \varepsilon = 0.01$

(a) the nullclines of model(6) (b) dynamical behaviours of model (6)

Model (6) was then discretised using the FTCS method, where a von Neumann neighbourhood was selected to describe the diffusion of the components and the temporal sampling constant and spatial sampling constant were set as $dt = 1$ and $dx = 1$. The other model parameters were set as $\varepsilon = 0.01, \alpha = 0.1$, $\beta = 0.5$, $\gamma = 1.6$, $\delta = 0$ and the diffusion coefficients of components u and v as $D_u = 0.2$ and $D_v = 0$. The simulation was run on a 200×200 lattice with a periodic boundary condition. The simulation started from a zero initial state disturbed by several bar-shaped noises with different values, which is shown as the first figure in Fig 2. The snap shots of the simulated pattern are shown in Fig 2. Typical spiral patterns were generated using model (6).

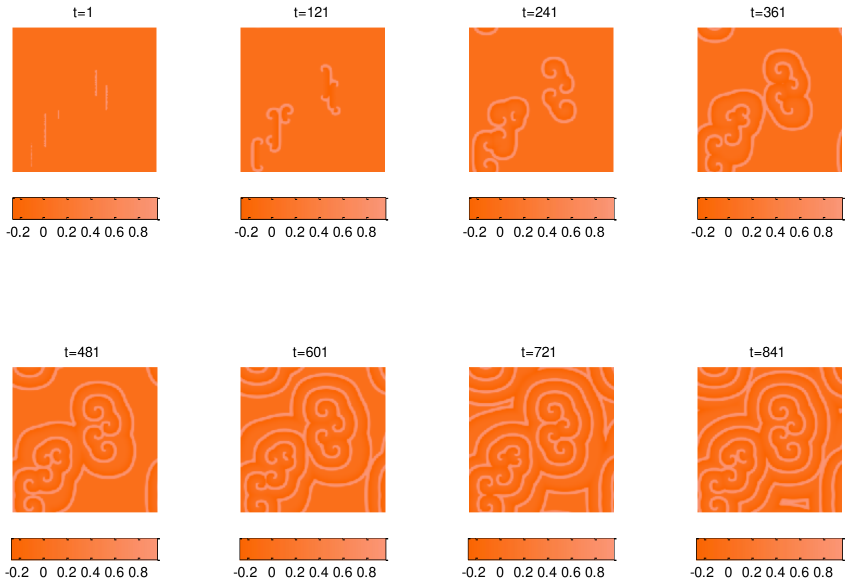

Fig 2 Simulation of the FHN model (component u)

$$dt = 1, dx = 1, \varepsilon = 0.01, \alpha = 0.1, \beta = 0.5, \gamma = 1.6, \delta = 0, D_u = 0.2, D_v = 0$$

For different choices of the parameters, model (6) can exhibit different spatio-temporal patterns. Keeping all the parameters fixed but resetting the parameter α to $\alpha = -0.1$, and simulating the FHN model on the same lattice with an initial condition given in the first figure of Fig 3 produced typical expanding target patterns. Snap shots of the simulated patterns are shown in Fig 3

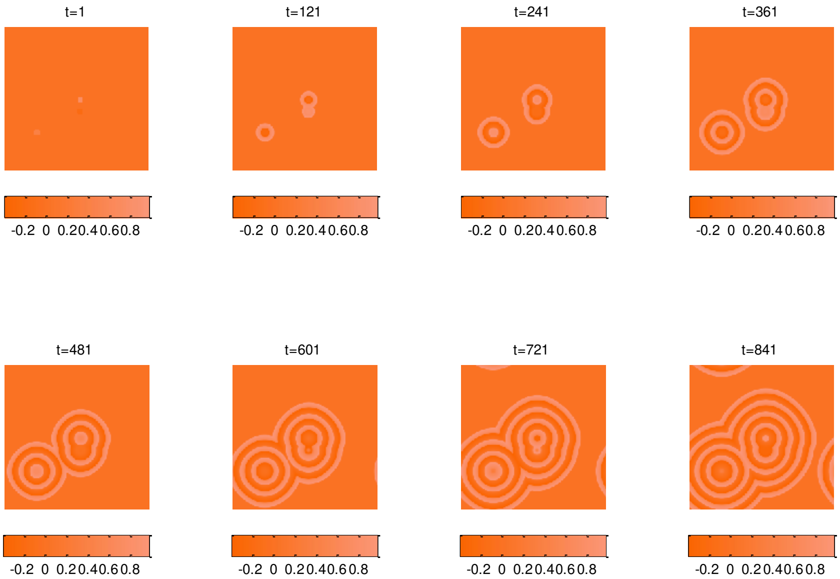

Fig 3 Simulation of the FHN model (component u)

$$dt = 1, dx = 1, \varepsilon = 0.01, \alpha = -0.1, \beta = 0.5, \gamma = 1.6, \delta = 0, D_u = 0.04, D_v = 0$$

2.3 Simulation of the Oregonator Model

The Oregonator Model was derived from the chemical kinetics of the famous Belousov-Zhabotinsky reaction and is widely used for the analysis of excitable media. A two component Oregonator model is given as

$$\begin{cases} \varepsilon u_t = D_u \nabla u + u(1-u) + f \dfrac{(q-u)}{(q+u)} w \\ w_t = D_w \nabla w + u - w \end{cases} \tag{7}$$

Set the parameters of the Oregonator model as $\varepsilon = 0.04, q = 0.008$ and $f = 2/3$, the diffusion coefficients as $D_u = 0.1$ and $D_w = 0$. Discretise the Oregonator model using $dt = 0.01, dx = 1$ and simulate the discrete model on a 200×200 square lattice. Using the first figure in Fig 4 as the initial condition where a zero initial condition is disturbed by some spot-shape noises, snap shots of the simulated pattern are shown in Fig 4. Target shaped patterns are produced and observed.

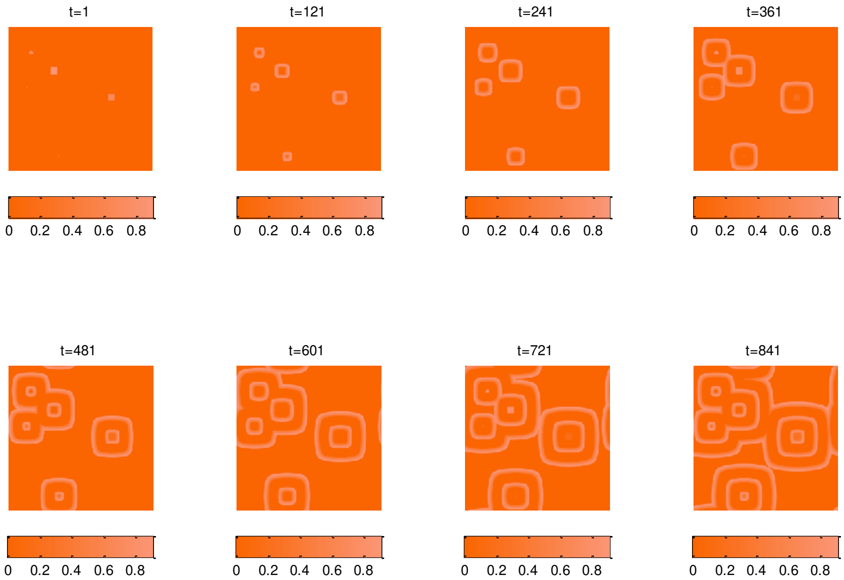

Fig 4 Simulation of the Oregonator model (component u)

$$dt = 0.01, dx = 1, \varepsilon = 0.04, q = 0.008, f = 2/3, Du = 0.1, Dw = 0$$

2.4 Simulation of Cellular Automata Model

The Greenberg-Hasting Model (GHM), which was introduced by Greenberg and Hasting (1978; 1978) is the most common CA form of model for excitable media. Recently, this model has be used to identify the BZ pattern by Zhao and Billings(2007a; 2007b). In this model, three key parameters can be controlled to generate complex patterns: the number of states, the number of excited states and the threshold for excitation.

For an n-state spatio-temporal system which is described using a GHM model, all the states, denoted as $\{0,1,\cdots,n-1\}$, are in one of the three states: excitable (resting), excited or refractory. Here, we use 0 to represent an excitable state, $n-1$ represents the excited state, and the states between the excitable state and excited state are refractory. Denote a cell at spatial coordinate (i, j) and the time step t as $c_{i,j}^t$ and the neighbourhood of the cell as $\chi(c_{i,j}^t)$. Define the number of excited cells in the neighbourhood as $\varepsilon(c_{i,j}^t)$.

The transition rule of the GHM model is given as

$$c_{i,j}^{t+1} = \begin{cases} c_{i,j}^t - 1 & if\ c_{i,j}^t > 0 \\ n-1 & if\ c_{i,j}^t = 0\ and\ \varepsilon(c_{i,j}^t) \geq n_e \\ 0 & otherwise \end{cases} \tag{8}$$

where n_e represents the threshold of excitation.

Set the number of states as 7 where state 0 represents the resting state, 2 ~ 5 the refractory state, and 6 represents the excited state. The threshold for excitation is set as 6, namely, an excitable cell changes its state to an excited state at the next step when there are at least 6 cells in its neighbourhood that are in an excited state. Here a Moore neighbourhood of range 3 was used, that is $\chi\left(c_{i,j}^t\right) = \left\{c_{k,l}^{t-1} : |k-i| \leq 3, |l-j| \leq 3\right\}$. This GHM model was simulated on a 200×200 square lattice with a periodic boundary condition. The simulation was started from a random initial condition and the generated pattern is shown in Fig 5. Typically spirals are observed in the simulated patterns.

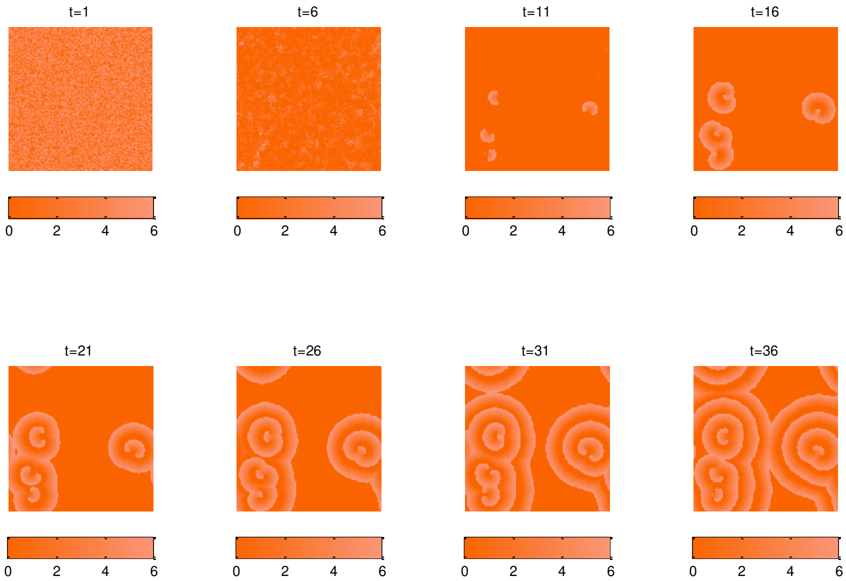

Fig 5 Simulated pattern of the GHM model

3. Scalar CML Model

In the last section, coupled PDEs and cellular automata were used to simulate excitable patterns. However both coupled PDEs and cellular automata may not be suitable for the identification of practical excitable media. Cellular automata models may be too simple to describe a practical system because only very limited parameters in the models can be identified.

Excitable media are most naturally represented as partial differential equations, where the evolution of cells in the excitable media is modelled by coupled differential equations. The number of differential equations required to represent a cell in the system may be large. For example, the DiFrancesco-Nobel model of Purkinje fibers has 14 dimensions and over a hundred parameters (Difrancesco and Noble 1985). In an excitable media model at least two components are needed: an excitation variable and a recovery variable, that is, **u** is a vector of at least two variables. Ignoring the effects of diffusion, the variables interact locally according to the ordinary differential equations

$$\frac{d\mathbf{u}}{dt} = \mathbf{f}(\mathbf{u}, \mathbf{p}) \tag{9}$$

For a variable u of vector $\mathbf{u}$, $\dot{u} = 0$ shows all the fixed points in the $u - \dot{u}$ plane. In an oscillatory pattern, another variable v is needed to drive u off the stable fixed points. Here, u is the excitation variable and v acts as the recovery variable.

Descretising the partial differential equations produces a coupled map lattice model (CML). A general CML model for an autonomous system can be expressed as

$$\boldsymbol{u}(t, \boldsymbol{x}) = f \quad p^{m_u} q^{n_u} \boldsymbol{u}(t, \boldsymbol{x}) \tag{10}$$

In the above equation, t is the one dimensional discrete temporal coordinate; $\boldsymbol{x}$ is a d dimensional discrete spatial coordinate; p and q are spatial and temporal shift operators (Billings and Coca 2002; Coca and Billings 2001). The discrete CML models usually have the same number of variables as the partial differential system.

Using these partial differential equations and coupled map lattice models in which several coupled components are included to identify a practical excitable media system, complete information about these coupled components should be measurable. However, for a practical system, only one component is measurable and the measured data denoted as z are usually a complex nonlinear function of the original component vector **u**, that is, $z = z(\mathbf{u})$.

In this section a new coupled map lattice model is introduced where only one measured component is used. The scalar coupled map lattice model (SCML) can be defined as

$$z(t) = f\left(p^{m_r} z, p^{m_d}\left(\nabla^2 z\right)\right) \tag{11}$$

In the above model, z represents the only component measured from practical patterns; p is a temporal shift operator; ∇^2 is the Laplace operator, which represents the diffusion of component z; f is a nonlinear function of z at previous times, and the diffusion of z at previous times.

To illustrate the existence of the SCML model, consider a two component reaction-diffusion system given in (12).

$$\begin{cases} u_t = D_u \nabla^2 u + f(u,v) \\ v_t = D_v \nabla^2 v + g(u,v) \end{cases} \tag{12}$$

In the first equation of (12) an implicit function from u to v exists. Give this function explicitly as

$$v = f_h\left(u, u_t, \nabla^2 u\right) \tag{13}$$

Calculating the first order temporal derivative yields

$$v_t = \frac{\partial}{\partial t} f_h\left(u, u_t, \nabla^2 u\right) = f_{ht}\left(u, u_t, \nabla^2 u, \left(\nabla^2 u\right)_t\right) \tag{14}$$

Substituting (13) and (14) into the second equation of (12) produces

$$f_{ht} = D_v \nabla^2\left(f_h\right) + g\left(u, f_h\right) \tag{15}$$

In equation (15), only component u and its temporal and spatial derivatives are included. Letting the measurement component $z = u$ yields what will be called a scalar coupled map lattice model.

Two examples, the FitzHugh-Nagumo model and the Oragonator model will be analysed. Firstly consider the FHN model given in equation (6). The first equation can be explicitly written as

$$v = D_u \nabla^2 u - u(u-1)(u-\alpha) - u_t \tag{16}$$

Calculating the first order time derivative of both sides produces

$$v_t = \left(D_u \nabla^2 u\right)_t - 3u^2 u_t + 2(1+\alpha) u u_t - \alpha u_t - u_{tt} \tag{17}$$

Substituting equation (16) and (17) into the second equation yields

$$
\begin{aligned}
&u_{tt} + \left(3u^2 - 2(1+\alpha)u + (\alpha + \varepsilon\gamma)\right)u_t + \varepsilon\gamma u^3 - \varepsilon\gamma(1+\alpha)u^2 \\
&+\varepsilon\left(\beta + \alpha\gamma\right)u - \varepsilon\delta - \left(D_u \nabla^2 u\right)_t = 0
\end{aligned}
\tag{18}
$$

Repeating the same process for the Oregonator model given in (7) yields the one component version of this model as

$$A_t B - AB_t - B^2 u + AB = 0 \tag{19}$$

where $A(u) = \varepsilon u u_t + \varepsilon q u_t + u^3 - (1-q)u^2 - qu - \left(D_u \nabla^2 u\right)(q+u)$ and $B(u) = (fq - fu)$.

The above analysis shows that a reaction-diffusion coupled PDE model can be rewritten in a one component form. Disceretising these continuous one component models yields the SCML models defined in (11). Although the scalar model which is derived from a simple mathematical development looks no different to the coupled PDEs, this kind of model has an important meaning for the identification of spatio-temporal patterns because for a practical spatio-temporal system not all the components which are involved in the evolution of a cell can be measured from the acquired data. For most practical spatio-temporal patterns, for example, the chemical BZ pattern or skin patterns on fishes and shells, only one component can be observed and the measured component may be a complex nonlinear function of those effects which actually affects the evolution of the patterns.

Simultaneously, the scalar models derived from the original PDEs also give some important guidance on the identification of the spatio-temporal patterns: (1) the terms with second order derivative should be included in the final model. That means terms with at least second order time-lags should be included in a discrete SCML model; (2) the spatial derivatives and the first order time derivative of these spatial derivatives should be included in the final model. That is, the diffusion term at time before *t-1* should be considered in an SCML model.

4 Identification of Excitable Media Patterns

The last section showed that a SCML model can be developed from coupled PDE forms of models. However, for experimental or naturally occurring excited media, even the PDE form of such models is often unknown. One reasonable method is to reconstruct the dynamics of multi-component systems directly from the observed patterns. Takens embedding theorem (1981) showed that $2n+1$ time-delayed versions of one observation function would suffice to embed an n-dimensional phase space. That is, an n-dimensional dynamical system can be reconstructed using only one observed variable and associated time delays. A similar idea can be used in the SCML model where both the time delays of the measurement variable and its diffusion are used. In this section the orthogonal least squares algorithm is employed as the main methodology to determine the structure of the SCML model and to estimate the associated parameters.

4.1 Identification of Simulated Patterns

In this section a 2-D simulated pattern is identified. The data used for the identification was generated by simulating the FitzHug-Nagumo model with $\alpha = 0.1, \beta = 0.5, \gamma = 1.6, \delta = 0, \varepsilon = 0.01$. The simulated pattern was sampled with the spatial and temporal sampling intervals $\Delta t = 2$ and $\Delta x = 1$. Fig 6 shows the snap shots of the sampled pattern.

Fig 6 The pattern generated using the FHN model (component u)

$$\alpha = 0.1, \beta = 0.5, \gamma = 1.6, \delta = 0, \varepsilon = 0.01$$

An SCML model was then used to identify this pattern. Select the measurement function as $z = u$. Assume the form of the function (11) is not known but that the function can be approximated by a third-order nonlinear polynomial form of model. Construct the 3rd-order nonlinear polynomial model set. A von Neumann neighbourhood was considered to describe the diffusion effects and a second order time lag was selected as discussed in the last section. The orthogonal least squares algorithm(Billings et al. 1989; Chen et al. 1989) was then applied to the data to select the significant model terms. The corresponding parameters are then estimated based on the selected terms. The identification results are given in Table 1. Notice that $\nabla^2 z(t-1)$ and $\nabla^2 z(t-2)$ have been selected as specific terms in the model as suggested by the analysis in section 3.

Table 1 Model selection for the FHN system

Terms	**ERR's**	**Coefficients**
$z(t-1)$	0.984331	1.7981
$z(t-2)$	0.013315	-0.82041
$\nabla^2 z(t-1)^a$	0.001306	0.459467
$\nabla^2 z(t-2)^b$	3.26E-05	-0.42561
$z^3(t-2)$	1.14E-06	1.65721
$z^2(t-2)$	2.47E-05	-1.83072
$z^2(t-1)$	1.87E-05	1.88849
$z^3(t-1)$	0.000861	-1.70921

[a] $\nabla^2 z_{i,j}(t-1) = \left(z_{i,j-1}(t-1) + z_{i,j+1}(t-1) + z_{i-1,j}(t-1) + z_{i+1,j}(t-1)\right)/4 - z_{i,j}(t-1)$

[b] $\nabla^2 z_{i,j}(t-2) = \left(z_{i,j-1}(t-2) + z_{i,j+1}(t-2) + z_{i-1,j}(t-2) + z_{i+1,j}(t-2)\right)/4 - z_{i,j}(t-2)$

The identified model can be written as follows

$$\begin{aligned} z(t) = {} & 1.7981 z(t-1) - 0.820409 z(t-2) + 1.65721 z^3(t-2) \\ & - 1.83072 z^2(t-2) + 1.88849 z^2(t-1) - 1.70921 z^3(t-1) \\ & + 0.459467 \nabla^2 z(t-1) - 0.42561 \nabla^2 z(t-2) \end{aligned} \tag{20}$$

Using the configuration at time instant t=60 and t=61 as the initial state of the system, the model predictions of model (20) are show in Fig 7. The predicted pattern is almost exactly the same as the original pattern generated using the FHN model equations even for t=300.

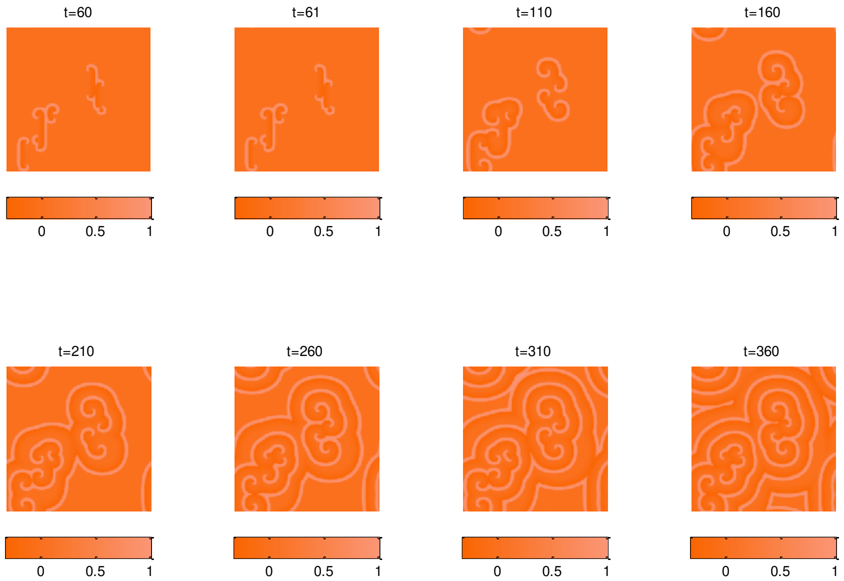

Fig 7 Model prediction output of SCML model (20)

4.2 Identification of a Practical Belousov-Zhabotinsky Pattern

The Belousov-Zhabotinsky (BZ) reaction has been widely used as a prototype system for the study of chemical oscillations and pattern formation for several decades. The BZ reaction-diffusion system has been utilised primarily to understand the dynamics of patterns consisting of travelling waves, including target patterns and spiral waves. Fig 8 shows snap shots of a pattern acquired from a real Belousov-Zhabotinsky reaction.

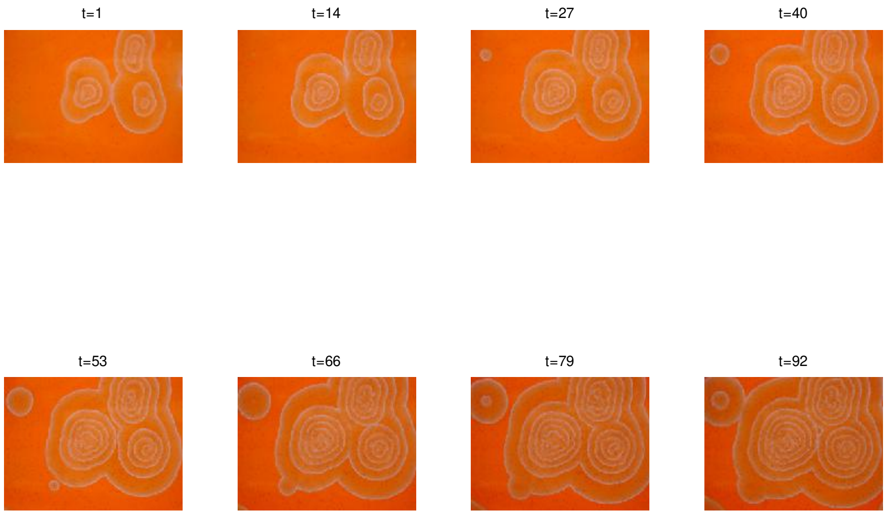

Fig 8 Snap shots of the acquired data

The experiments were completed by Dr. Y. Zhao with collaborators from colleagues in the Chemical Engineering Department. The patterns acquired from the practical BZ reaction are stored as RGB images. An $L \times W$ pixel image is an $L \times W \times 3$ data array that defines red, green and blue colour components for each individual pixel. Selecting a cell from the pattern, Figure 9 shows the changes of colour components over time at this point. These lines represent the dynamical changes of the cell state.

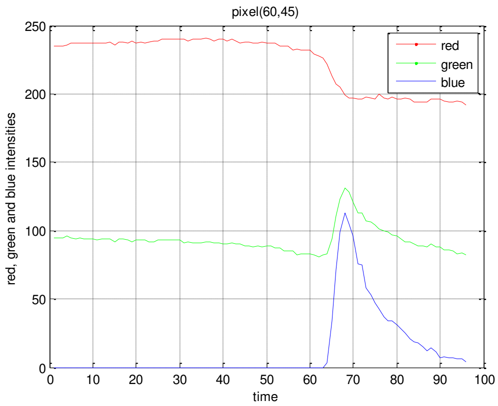

Fig 9 Red, green and blue colour component of a pixel in the BZ reaction

In Fig 9, the blue intensity of the cells lays out a similar shape as the local dynamics in an excitable medium. Accordingly the blue component of the acquired pattern is selected as the measurement component z for the identification. Snap shots of the blue component of the acquired pattern are given in Fig 10. Part of the blue component data were then used for the identification and the first two figures in Fig 11 were used as the initial states for the model prediction.

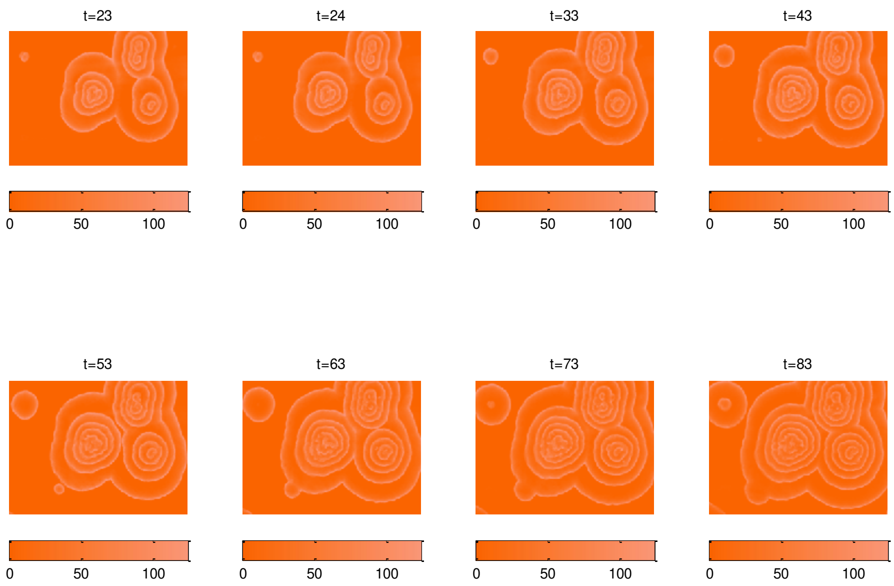

Fig 10 Blue component of the acquired BZ patterns

Because the patterns were severely noisy from the experimental environment together with occasional bubbles which were generated in the chemical reaction, not all the data can be used for the identification. A method has to be introduced to select good data which can be used. Selecting two data sets, denoted as data set (a) and date set (b), from the blue component pattern. The phase portraits of the two data sets are plotted in Fig 11. For the data set (a) there appears to be no clear functional relationship, or if there is it is extremely noisy, while data set (b) shows a clearer relationship between $z(t)$, $z(t-1)$ and $z(t-2)$. In other words, it is more likely that a function $z(t) = f\left(z(t-1), z(t-2)\right)$ can be found from data set (b) than from data set (a). Consequently, the phase portrait can be used for the selection of the data set. Data set (b) was selected for the identification of the model.

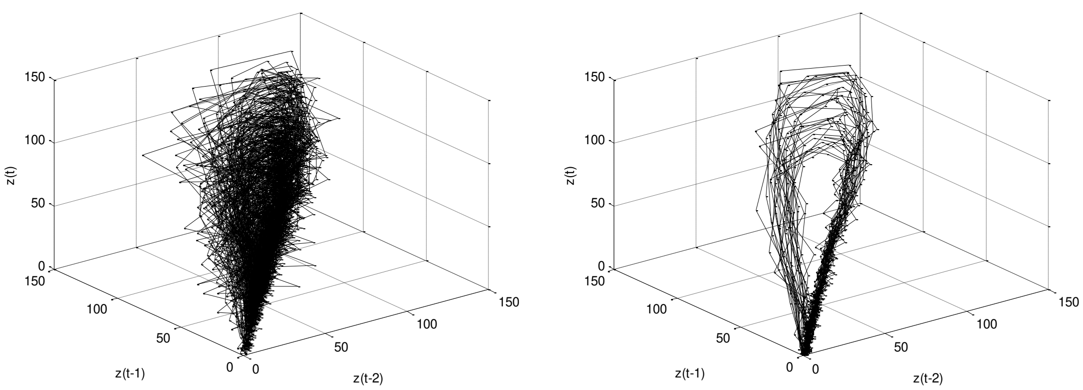

(a) (b)

Fig 11 Data collected from the acquired B-Z pattern

(a) The improperly chosen data (b) The properly chosen data

The SCML model was used to identify the practical pattern. Obviously we have no idea about the structure of the model because this is a real data set. Assume the model can be approximated by a fourth-order polynomial model and construct the fourth-order nonlinear model set. A von Neumann neighbourhood was used to describe the diffusion of the components. Following the reasoning from the last section, a second-order time lag of the cell states and the diffusion was considered. Applying the orthogonal least squares algorithm to data set (b), the most significant terms were selected from the fourth-order full term set. The results are shown in Table 2.

Table 2 Model selection for the BZ system

Terms	**ERR's**	**Coefficients**
$z(t-1)$	0.95414	0.95013
$z(t-2)$	0.0224055	-0.0424791
$\nabla^2 z(t-1)^a$	0.0085178	0.743265
$z^4(t-1)$	0.000947576	1.86899E-05
$z^3(t-1)z(t-2)$	0.00332102	-5.73529E-05
$\nabla^2 z(t-2)^b$	0.00018247	-0.354318
$z^2(t-1)z^2(t-2)$	0.000055963	6.28918E-05
$z^3(t-1)$	8.25933E-06	-0.00310803
$z^2(t-1)$	0.000166008	0.118357
$z(t-1)z(t-2)$	4.36405E-05	-0.185982
$z^2(t-1)z(t-2)$	0.000953827	0.00779509
$z^4(t-2)$	5.29455E-05	3.0084E-06

$z(t-1)z^3(t-2)$	0.00014928	-2.71051E-05
$z(t-1)z^2(t-2)$	4.19106E-05	-0.0068082
$z^3(t-2)$	0.00104672	0.00207884
$z^2(t-2)$	0.000561697	0.0712825

[a] $\nabla^2 z_{i,j}(t-1) = \left(z_{i,j-1}(t-1) + z_{i,j+1}(t-1) + z_{i-1,j}(t-1) + z_{i+1,j}(t-1)\right)/4 - z_{i,j}(t-1)$

[b] $\nabla^2 z_{i,j}(t-2) = \left(z_{i,j-1}(t-2) + z_{i,j+1}(t-2) + z_{i-1,j}(t-2) + z_{i+1,j}(t-2)\right)/4 - z_{i,j}(t-2)$

The final SCML model is given as

$$\begin{aligned} z(t) &= 0.95013z(t-1) - 0.0424791z(t-2) + 0.743265\nabla^2 z(t-1) \\ &+ 1.86899\times10^{-5} z^4(t-1) - 5.73529\times10^{-5} z^3(t-1)z(t-2) \\ &- 0.354318\nabla^2 z(t-2) + 6.28918\times10^{-5} z^2(t-1)z^2(t-2) \\ &- 0.00310803z^3(t-1) + 0.118357z^2(t-1) - 0.185982z(t-1)z(t-2) \\ &+ 0.00779509z^2(t-1)z(t-2) + 3.0084\times10^{-6} z^4(t-2) \\ &- 2.71051\times10^{-5} z(t-1)z^3(t-2) - 0.0068082z(t-1)z^2(t-2) \\ &+ 0.00207884z^3(t-2) + 0.0712825z^2(t-2) \end{aligned} \tag{21}$$

Ignoring the diffusion part of model (21), the local dynamics of the SCML model is shown in Fig 12. Because the model does not include a constant term, the state of cell $z(t)$ will remain zero (the resting state) when a zero initial condition is set. For a small perturbation, the state of the system is damped out while a perturbation which is large enough triggers a long excursion and finally a return to the resting state. The excited curve has a similar shape and amplitude to the blue curve in Fig 9.

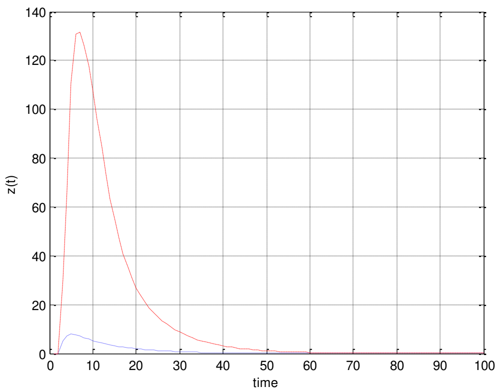

Fig 12 Local dynamics of the identified model

Using the configurations at t=23 and t=24 as the initial conditions, the model prediction output patterns are shown in Fig 13. Compared with the practical pattern in Fig 10, the long time predicted pattern keeps the same shape and a similar propagation speed.

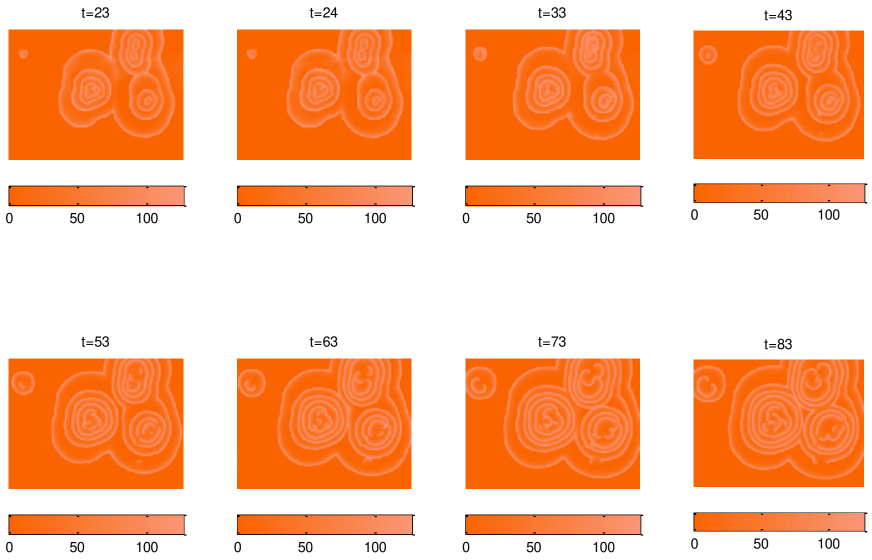

Fig 13 Model prediction output of model (21)

When the identified SCML model is simulated on a 240×180 square lattice with a zero-flux boundary condition starting from a random initial state, typical spiral patterns are observed in the patterns which are shown in Fig 14. By slightly changing the parameters, this model can exhibit various spatio-temporal patterns.

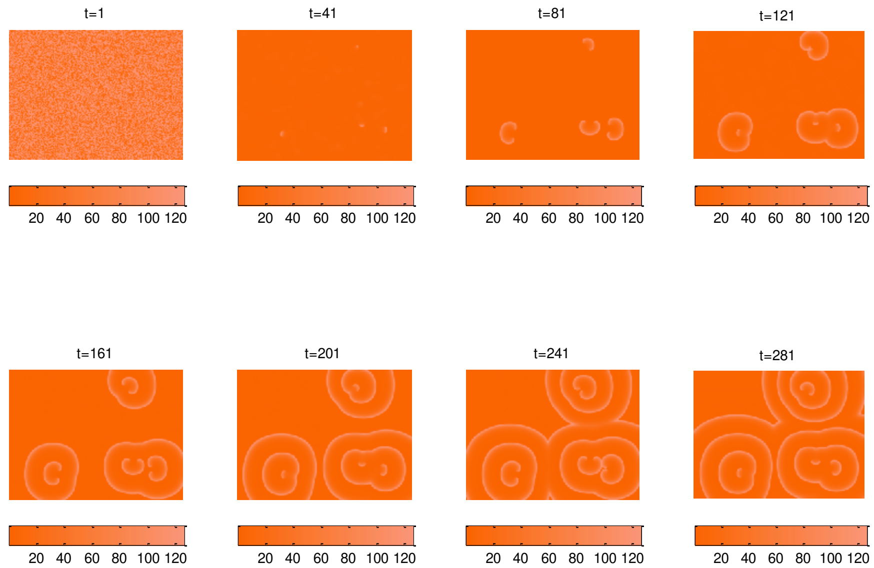

Fig 14 Simulation of SCML model (21)

5 Conclusions

As an important class of spatio-temporal system, excitable media have received a lot of attention. In this paper, a scalar coupled map lattice (SCML) model was for the first time proposed to identify this class of spatio-temporal systems. Both simulated patterns and real practical patterns observed from a real BZ chemical reaction were successfully identified by applying the OLS algorithm to the new SCML models. The identified SCML models appear to possess the same local dynamical features as the original patterns and are able to generate target patterns and spirals which are commonly observed in excitable media.

The identification of the SCML model directly from an observed pattern led to many interesting observations. Firstly, the identification process demonstrated that the full details of real dynamics of spatio-temporal systems are not necessary to identify a microscopic model with similar macroscopic behaviours. Secondly, the SCML model provides an alternative choice for the numerical simulation of excitable media besides partial differential equations and cellular automata. Thirdly, the identification method builds a direct connection between practical systems and models. Although only travelling wave patterns have been considered in this chapter, the method may also be used for the identification of stationary patterns, such as Turing patterns.

Acknowledgment

The authors gratefully acknowledge support from the UK Engineering and Physical Sciences Research Council (EPSRC) and the European Research Council (ERC).

References

Billings, S. A., Chen, S., and Korenberg, M. J. (1989). "IDENTIFICATION OF MIMO NON-LINEAR SYSTEMS USING A FORWARD-REGRESSION ORTHOGONAL ESTIMATOR." *International Journal of Control*, 49(6), 2157-2189.

Billings, S. A., and Coca, D. (2002). "Identification of coupled map lattice models of deterministic distributed parameter systems." *International Journal of Systems Science*, 33(8), 623-634.

Chen, S., Billings, S. A., and Luo, W. (1989). "ORTHOGONAL LEAST-SQUARES METHODS AND

THEIR APPLICATION TO NON-LINEAR SYSTEM-IDENTIFICATION." *International Journal of Control*, 50(5), 1873-1896.

Coca, D., and Billings, S. A. (2001). "Identification of coupled map lattice models of complex spatio-temporal patterns." *Physics Letters, Section A: General, Atomic and Solid State Physics*, 287(1-2), 65-73.

Difrancesco, D., and Noble, D. (1985). "A MODEL OF CARDIAC ELECTRICAL-ACTIVITY INCORPORATING IONIC PUMPS AND CONCENTRATION CHANGES." *Philosophical Transactions of the Royal Society of London Series B-Biological Sciences*, 307(1133), 353-398.

FitzHugh, R. (1955). "Mathematical models of threshold phenomena in the nerve membrane." *Bulletin of Mathematical Biology*, 17(4), 257-278.

Greenberg, J. M., Hassard, B. D., and Hastings, S. P. (1978). "PATTERN FORMATION AND PERIODIC STRUCTURES IN SYSTEMS MODELED BY REACTION-DIFFUSION EQUATIONS." *Bulletin of the American Mathematical Society*, 84(6), 1296-1327.

Greenberg, J. M., and Hastings, S. P. (1978). "SPATIAL PATTERNS FOR DISCRETE MODELS OF DIFFUSION IN EXCITABLE MEDIA." *Siam Journal on Applied Mathematics*, 34(3), 515-523.

Jankowski, S., and Wanczuk, R. "CNN models of complex pattern formation in excitable media." *Cellular Neural Networks and their Applications, 1994. CNNA-94., Proceedings of the Third IEEE International Workshop on*, 333-338.

Kaneko, K. (1990). "Simulating Physics with Coupled Map Lattices ".

Maini, P. K., Painter, K. J., and Chau, H. N. P. (1997). "Spatial pattern formation in chemical and biological systems." *Journal of the Chemical Society-Faraday Transactions*, 93(20), 3601-3610.

Pan, Y., and Billings, S. A. (2008). "The identification of complex spatiotemporal patterns using Coupled Map Lattice models." *International Journal of Bifurcation and Chaos*, 18(4), 997-1013.

Takens, F. (1981). "Detecting strange attractors in turbulence." Dynamical Systems and Turbulence, Warwick 1980, 366-381.

Wei, H. L., Billings, S. A., Zhao, Y. F., and Guo, L. Z. (2009). "Lattice Dynamical Wavelet Neural Networks Implemented Using Particle Swarm Optimization for Spatio-Temporal System Identification." *IEEE Transactions on Neural Networks*, 20(1), 181-185.

Zhao, Y., Billings, S. A., and Routh, A. F. (2007a). "Identification of excitable media using cellular automata models." *International Journal of Bifurcation and Chaos*, 17(1), 153-168.

Zhao, Y., Billings, S. A., and Routh, A. F. (2007b). "Identification of the Belousov-Zhabotinskii reaction using cellular automata models." *International Journal of Bifurcation and Chaos*, 17, 1687-1701.

Zykov, V. S. (2008). "Excitable media." *Scholarpedia*, 3(5), 1834.